Sensors and Actuators A xxx (2012) xxx–xxx

Contents lists available at SciVerse ScienceDirect

Sensors and Actuators A: Physical

journal homepage: www.elsevier.com/locate/sna

# Micromachined Pt–Rh and stainless steel relays for high power DC applications

Fatih M. Ozkeskin[a,*], Yogesh B. Gianchandani[a,b]

[a] Department of Mechanical Engineering, University of Michigan, Ann Arbor 48109, United States
[b] Department of Electrical Engineering and Computer Science, University of Michigan, Ann Arbor 48109, United States

ARTICLE INFO

*Article history:*
Received 13 September 2011
Received in revised form
16 December 2011
Accepted 18 December 2011
Available online xxx

*Keywords:*
Micro-relay
Heat sink
Cantilever
Pt–Rh

ABSTRACT

This paper explores the viability of bulk metal foils, in particular platinum–rhodium (Pt–Rh), for use in high power micromechanical relays. The electrical and thermal response of electrostatically actuated three-terminal micro-relays is evaluated. The micro-relays have a footprint of 6.5 $mm^2$ and an actuation area of 1.32 $mm^2$. A stacked double cantilever structure isolates the actuation electrode from the current path. A micromachined heat sink is located on the upper cantilever. The devices are fabricated by micro-electrodischarge machining and directly assembled on power rated printed circuit boards. The impact of contact materials, and forced cooling is addressed. Preliminary results suggest that the Pt–Rh devices have total on-state resistances of 1.25 Ω and can handle currents substantially in excess of 1 A, and potentially in excess of 2.6 A.



## 1. Introduction

The uses of micro-relays range from common DC applications in industrial machinery and automotive control circuits to high frequency signal switching applications such as in the aerospace sector, radio frequency (RF) communications and portable electronics [1–4]. Although significant attention has been devoted to the longevity of relays and switches, the focus has been primarily directed at devices handling relatively low levels of power [5]. High power handling in MEMS switches is of interest for power conversion, transmitters in satellites, and earth-based communications stations [6,7]. For switches that offer capacitive paths (used with RF signals), power handling is primarily affected by dielectric charging, whereas for DC-contact switches the microwelding of contact surfaces due to localized contact heating is the predominant failure mode. The power handling capability of such relays is strongly related to the nature of the contact metals [8,9].

Past work in DC micro-relays focused on design configurations [10–12] and several novel contact materials for increased power handling [13,14]. Most of the efforts were directed at surface micromachining techniques. These techniques restrict the use of metal alloys to those that can be sputtered as thin films [15,16]. Subtractive bulk micromachining of metal alloy foils offers a complementary approach.

Platinum–rhodium (Pt–Rh) is a chemically inert and mechanically robust hard metal alloy that is used for making high quality crucibles. These properties are appealing for high power micro-relays which require mechanical, electrical, chemical, and thermal integrity. Platinum group contact metals are known to significantly reduce stiction [17,18]. In addition, Pt–Rh alloy with 20% Rh content has much higher hardness and a higher melting point than pure platinum [19,20].

This paper describes the evaluation of Pt–Rh and stainless steel as micro-relays material using three-terminal test structures. The design of the test structure is intended for evaluation of the alloy material and design concepts; it is not intended for large scale production. A secondary goal is to evaluate the possible utility of an on-device heat sink.[1] Section 2 describes the micro-relay design, and Section 3 details the fabrication and assembly processes for the device. The experimental setup and results are presented in Section 4. These include electrical characterization, thermal performance, and preliminary lifetime tests for the device. The discussion and conclusions are provided in Section 5.

## 2. Design

The micro-relay utilizes a three-terminal source-gate-drain structure (Fig. 1(a)). The design has a footprint of 2.6 mm × 2.5 mm and it employs vertically stacked components that are directly assembled on a printed circuit board (PCB). The PCB uses a

* Corresponding author at: 1301 Beal Ave. EECS. Building 2423, Ann Arbor, MI 48109, United States. Tel.: +1 979 218 1087; fax: +1 734 763 9324.
*E-mail address:* ozkeskin@umich.edu (F.M. Ozkeskin).

[1] Portions of this work have been reported in conference abstract form in [21].

0924-4247/$ – see front matter © 2012 Elsevier B.V. All rights reserved.
doi:10.1016/j.sna.2011.12.033

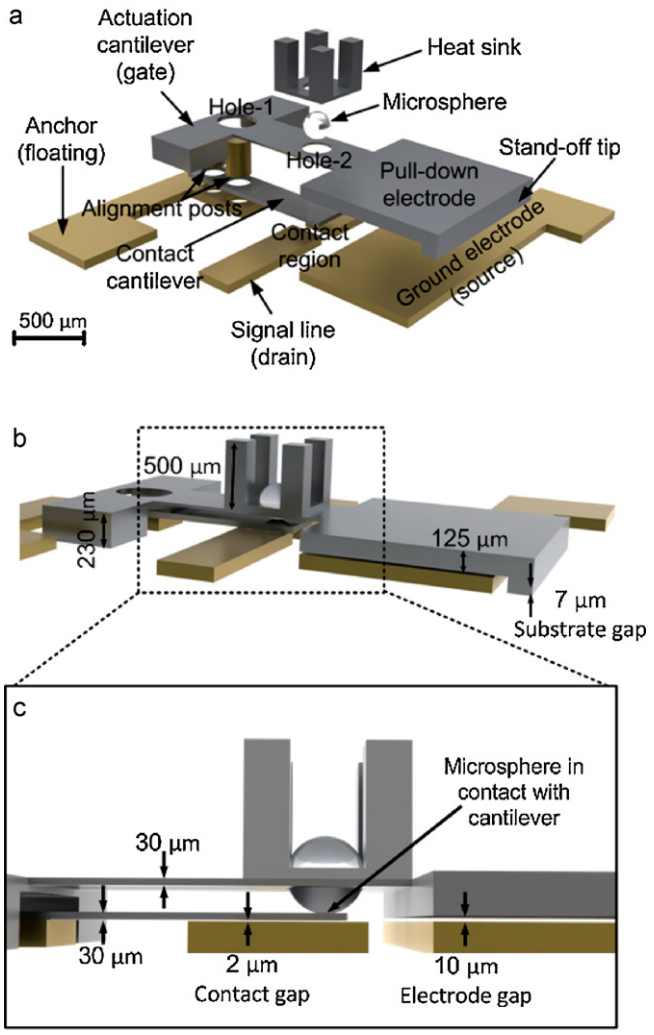


**Fig. 1.** (a) Exploded view of micro-relay showing double cantilever structure. Gold posts align and hold the cantilever over gold-coated copper traces on the PCB. A recess depth of 2 μm defines the contact gap on the contact cantilever. The actuation cantilever is isolated from contact cantilever and pushes it down via thermally conductive microsphere. An extension at the tip prevents pull-in. The heat sink is integrated atop. The design has an actuation area of 1.32 $mm^2$ as defined by the footprint of the pull down electrode (1200 μm × 1100 μm). (b) Isometric view and (c) side view of the cantilevers showing critical gaps for electrostatic actuation and pull-in prevention.

1.6 mm-thick standard FR-4 substrate. Interconnect traces of 90 μm thickness Cu were chosen for high current ratings – 4.5 A for 400 μm wide signal lines. In such PCBs, a 4 μm thick Ni layer covers the Cu traces, and a 0.15 μm thick outer gold layer provides the contact surface. The layout has three distinct regions: a ground electrode which acts as the source; an open signal line with a break in the middle which acts as the drain; and an electrically floating anchor pad with through vias, which accommodates the alignment and the placement of components to construct the micro-relay.

A contact cantilever (400 μm × 1400 μm × 30 μm including anchor; 600 μm suspended length), is located orthogonally with respect to the signal line and suspended above the break. Two alignment posts, extending from the vias, perforate the contact cantilever and fix it to the anchor on the PCB. The underside of the contact cantilever has 2 μm recess, over the signal line, to provide with an initial gap (Fig. 1(b) and (c)).

The actuation cantilever (1200 μm × 2100 μm × 230 μm including anchor; 1500 μm suspended length) is attached directly on the PCB substrate and suspended above the contact cantilever.

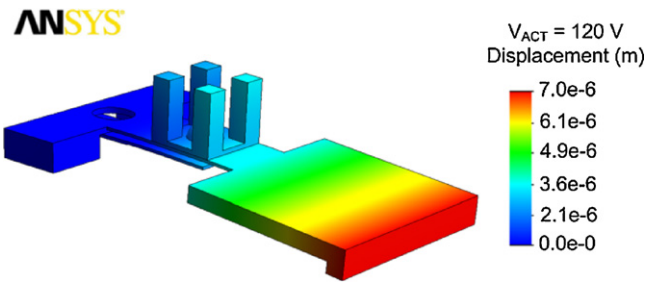


**Fig. 2.** Electrostatic FEA showing displacement results for micro-relay. $V_{ACT}$ is electrostatic actuation voltage (120 V) applied on the pull-in electrodes to cause cantilevers to travel 7 μm, before stopped by the stand-off tip. Simulated contact force and actuation time are 1.1 mN/contact region and 9.4 ms, respectively, for an increased voltage of 150 V.

A paddle shaped extension at the distal end acts as a gate pull-in electrode (with 1200 μm × 1100 μm actuation area) and allows electrostatic actuation when biased with respect to the electrode below it. A stand-off element extends from the tip of the actuation cantilever. The gap between the stand-off tip and the substrate is designed to be 7 μm–3 μm smaller than the electrode gap across the actuation cantilever and ground electrode as illustrated in Fig. 1(b). (It is recognized that in an environment that is not clean an electrically insulating layer will be necessary to prevent inadvertent shorting of the actuation electrodes.) *Hole-1* on the actuation cantilever prevents contact with the alignment posts, whereas *hole-2* accommodates subsequent placement of a microsphere.

A thermally conductive sapphire microsphere (Edmund Optics, 300 μm diameter, 45 $W K^{-1} m^{-1}$ thermal conductivity) is used on the contact cantilever. It fits tightly in *hole-2* which has the same diameter. The microsphere mechanically couples the actuation cantilever with the contact cantilever while keeping it electrically separated. It provides a single point of contact between the actuation cantilever and the contact cantilever, partially alleviating any assembly imperfections. In addition, it provides a thermal conduction path to dissipate heat away from the electrical contact region.

An aluminum heat sink (500 μm × 500 μm × 500 μm, 475 μm fin height) is located above the actuation cantilever. A through-hole at the base of the heat sink, concentric with *hole-2* on the actuation cantilever, supports the microsphere and provides a heat dissipation path from contacts to the heat sink fins. The efficiency of the designed fin is 0.812 for a fin height of 475 μm. Further details are provided in [22].

Results from the electrostatic-mechanical modeling of the micro-relay are shown in Fig. 2. The simulations were carried out in ANSYS. The pull-in voltage for a 7 μm vertical tip displacement was 120 V; at this point the stand-off tip touched the substrate. The spring constant for the device with combined cantilever pair, heat sink and the microsphere, was 56 N/m. The contact force per contact region was 1.1 mN for 150 V actuation voltage; the switching time was 9.4 ms.

Thermal modeling for contact heat dissipation and forced cooling requires a good estimate of the contact resistance to account for joule heating. Holm's well known plastic deformation model [23] was initially used to estimate the contact resistance. The model suggests that:

$$F = A_C H n \quad (1)$$

where $F$ is the contact force, $A_C$ is the actual mechanical contact area of overlapping contact asperities between touching surfaces, $H$ is the contact metal hardness, and $n$ is an empirical factor which

Please cite this article in press as: F.M. Ozkeskin, Y.B. Gianchandani, Micromachined Pt–Rh and stainless steel relays for high power DC applications, Sens. Actuators A: Phys. (2012), doi:10.1016/j.sna.2011.12.033

depends on material and approaches 1 for clean surfaces. Incorporating contact radius into this model gives:

$$\alpha_H = \sqrt{\frac{F}{Hn\pi}} \quad (2)$$

where $\alpha_H$ is the radius of Holm's contact spot (α-spot) representing a cluster of multiple small contact spots. Contact radius $\alpha_H$ can be used to estimate the Maxwell spreading resistance between two contacting surfaces assuming that the contact radius is much larger than the electron mean free path length of contacting materials. This spreading resistance is also known as constriction resistance.

$$R_{C\_theory} = \frac{\rho_1 + \rho_2}{4\alpha_H} \quad (3)$$

Here, $\rho_1$ and $\rho_2$ are the electrical resistivities of the contacting metals [24]. Adopting the contact mechanism proposed in [25], it can be assumed that contact pressures on a pair of asperities are equal to the flow pressure of the softer of the two contacting materials and that the normal load is supported by plastic flow of the softer asperities of that pair. However, it is important to note that in a multilayered structure the effective hardness is affected not only by the hardness of the top layer, which is thin in this case, but also by the hardness of thicker bottom layer material. Determining an exact value for hardness in the multilayered Cu/Ni/Au patterns used for the PCB traces is nontrivial and tabulated values for specific multilayer films are not readily available. The contact resistance modeling of sputtered films with different thicknesses and its mismatch with Holm's theory has been previously reported [26]. Since the thickness of the Ni layer (4 μm) is substantially larger than the thickness of the Au (0.15 μm), the effective hardness was chosen as that of Ni. Using Eqs. (2) and (3), a theoretical contact resistance, $R_{C\_theory}$, of 620 mΩ was found for the micro-relay design, with an estimated contact hardness of 6 GPa – the approximate Meyer hardness of Ni, unity $n$, approximate combined resistivity of 30 μΩ cm for Pt–Rh, Cu/Ni/Au contacts, and 1.1 mN contact force per contact region (estimated by FEA for 150 V actuation voltage). The theory suggests 241 nm radius for α-spot.

The contact resistance was also estimated empirically. The experiment followed a procedure similar to the one described in [26]. It involved manually placing a machined Pt–Rh beam, with the intended dimensions of contact cantilever, against open signal lines, and then applying a controlled contact force. The contact force was supplied by a precision force gauge (Aurora Scientific, Model 403A). The gauge was mounted on a motorized $x$–$y$–$z$ stage and brought into close proximity to the Pt–Rh beam. The force was applied over a 1 mm contact diameter, in 200 μN increments, up to 2.2 mN. The test current was sourced at a level of 5 mA, while contact resistance was measured using a 4-wire technique. The total series empirical resistance, $R_{C\_emp}$, was 0.8 Ω for 2.2 mN total contact force that was distributed evenly over two contact regions. The empirical method estimates an α-spot of 186 nm radius. The change of contact resistance with the contact force and its comparison to Holm's model is shown in Fig. 3. The $R_{C\_emp}$ was larger than $R_{C\_theory}$ by approximately 25%.

The $R_{C\_emp}$ was used to determine joule heating boundary condition in the finite element model for contact heat dissipation. The adhesive between microsphere, actuation cantilever and heat sink was thermally modeled as an overlapping shell only around the microsphere with a thermal conductivity of 5 W/m K following the specifications of commercially available epoxy (Aavid Thermalloy). To model the forced cooling via a commercially available mini-fan (Sunon-UF3A3), an upward air flow of 0.22 m/s was used. (The flow rate was experimentally verified in air, at atmospheric pressure, using particle image velocimetry.) The modeled flow was constrained in a cylindrical box of 1.5 mm height and 1 mm diameter enclosing the contact area and the heat sink. Thermal

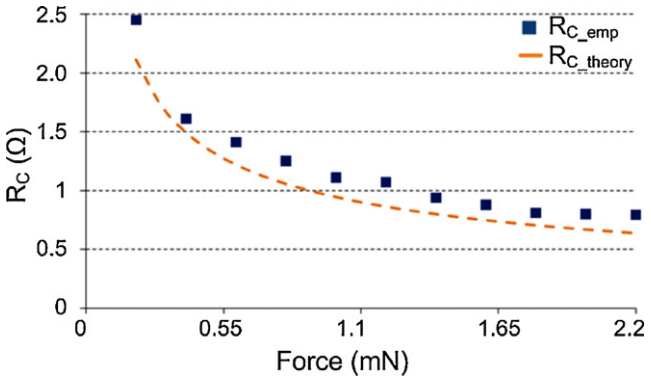


**Fig. 3.** Preliminary estimation of total series contact resistance with for use in the thermal model. Experimental plot showing the change of contact resistance with increasing force supplied from a force gauge on a Pt–Rh contact cantilever. The force was supplied in 200 μN increments, up to 2.2 mN total force (to obtain 1.1 mN force equally per contact area). The $R_{C\_emp}$ data is compared with $R_{C\_theory}$. For 2.2 mN, $R_{C\_emp}$ was 0.8 Ω whereas $R_{C\_theory}$ was 0.62 Ω.

finite-element analysis was performed in ANSYS. For both unforced and forced cooling, the temperature distribution was estimated at 1-s into the on-state. Fig. 4 shows the temperature distribution obtained for unforced and forced cooling for 2.5 A line current, 0.8 Ω $R_{C\_emp}$ and 300 K ambient temperature. Forced cooling decreases the maximum temperature in the contact area by approximately 25 K.

## 3. Fabrication and assembly

Micro-electrodischarge machining (μEDM) provides a lithography-compatible, subtractive manufacturing method for bulk metal foil devices with feature sizes as small as 5 μm. Feature patterning is possible in serial mode as well as in batch-mode. Batch mode μEDM uses a lithographically patterned chip – typically with electroplated Cu features on oxidized Si substrates – as a "cookie-cutter," to machine the workpiece [27]. In this effort, contact cantilevers for the micro-relay were machined using

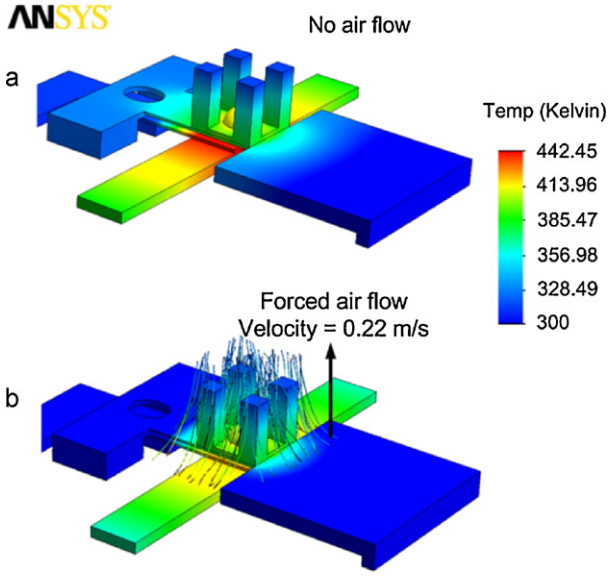


**Fig. 4.** FEA results at 1-s into the on-state time with 0.22 m/s upward air flow. Temperature distribution results for (a) unforced (b) forced cooling (Pt–Rh contact cantilever, 0.8 Ω $R_{C\_emp}$, 2.5 A line current, 300 K ambient temperature). Compared to unforced cooling, forced cooling suppresses temperature at contact region by around 25 K.

Please cite this article in press as: F.M. Ozkeskin, Y.B. Gianchandani, Micromachined Pt–Rh and stainless steel relays for high power DC applications, Sens. Actuators A: Phys. (2012), doi:10.1016/j.sna.2011.12.033

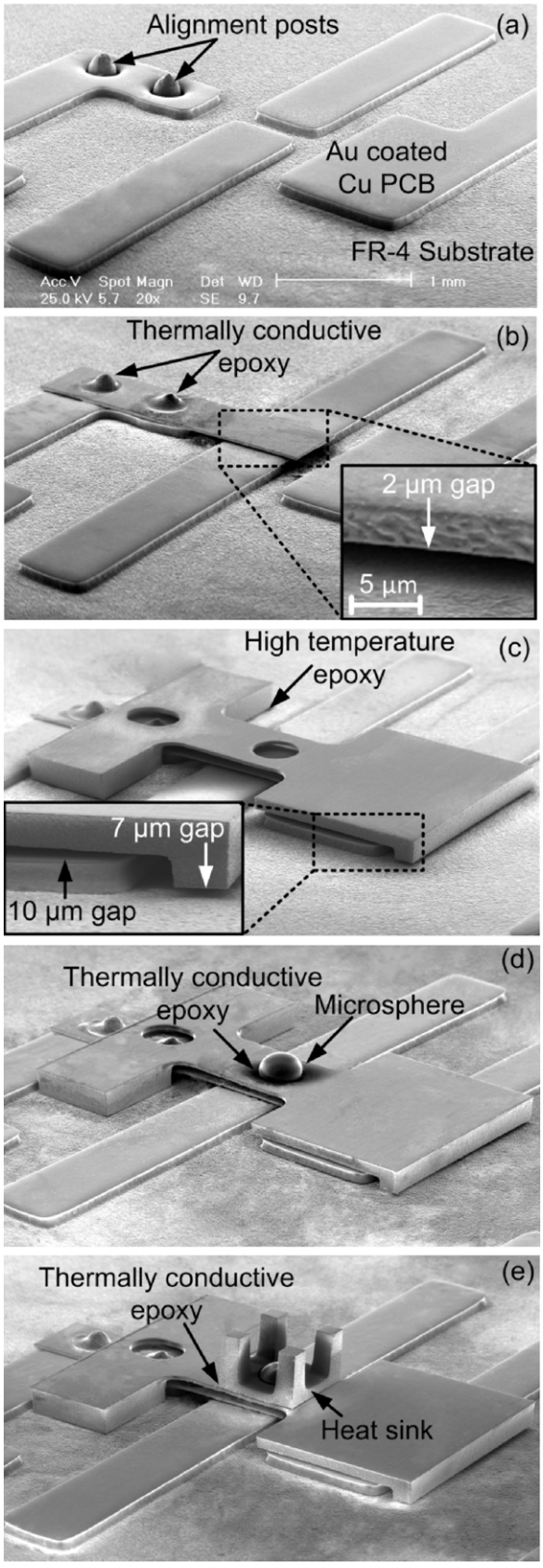


**Fig. 5.** SEM micrographs of assembly sequence for all-metal micro-relays showing: (a) floating anchor with alignment posts inserted. (b) Contact cantilever (Pt–Rh or SS316L) aligned on top of the posts through perforations and anchored with thermally conductive epoxy. Contact gap of 2 μm is shown. (c) Actuation cantilever directly placed on PCB substrate. Stand-off tip prevents electrostatic pull-in. (d) Microsphere inserted into the *hole-2*, secured with thermally conductive epoxy. (e) Heat sink placed by aligning the center hole around the microsphere, fixed with epoxy.

μEDM from both Pt–Rh (80:20) and SS316L alloys using 50 μm thick stock metal foils (Alfa Aesar Corp.).

Contact cantilevers were machined down to 30 μm thickness on anchors and 28 μm thickness over contact regions to allow for the 2 μm contact gap. Two perforations of 300 μm were located in anchor regions for attachment to the PCB via alignment posts. The lowest available discharge energy of 24.5 nJ was used for cantilever contact regions to ensure smooth surface finish and minimum residual stress. The surface roughness of the bottom side of both Pt–Rh and SS316L contact cantilevers was measured using Zygo NewView 5000 interferometer. Average roughness $R_a$ was approximately 45 nm for both cantilevers. In comparison, the virgin material had average roughness $R_a$ 25 nm.

The actuation cantilevers were machined using μEDM from hardened Al alloy 3003, using 250 μm thick stock foil. Compared to stainless steel, the higher thermal conductivity of Al can help dissipate heat. Initially, these cantilevers were machined down to 230 μm thickness. The pull-in electrode, and mid-section, where *hole-2* is located, was further reduced in thicknesses down to 125 μm and 30 μm, respectively. The perforations, *hole-1* and *hole-2* were then machined, similar to the perforations on the contact cantilevers. The heat sinks were machined using μEDM from 500 μm thick Al alloy 3003 foil.

Device assembly was performed by manual pick-and-place of components using tweezers. Gold wire alignment posts (1750 μm height; 300 μm diameter), were fitted into the PCB vias (Fig. 5(a)). Conical tip shapes allowed easy insertion and assembly. The length of the posts was designed to extend above the PCB trace by approximately 60 μm, to precisely accommodate the cantilevers. For the attachment of the contact cantilever to the electrically floating anchor pad, thermally conductive epoxy was manually applied through a syringe to ease heat dissipation through the posts (Fig. 5(b)). The epoxy was applied only between the alignment posts and the sidewalls of the holes on the contact cantilever. High viscosity thermally conductive epoxy (33,000 cps) prevented capillary flow and thickening underneath the cantilever and change in contact gap. To further maintain the contact gap during assembly, the contact cantilever was clamped in place while the epoxy was curing. Subsequently the actuation cantilever was assembled on top of the contact cantilever and attached to the substrate using high temperature epoxy (Cotronics Duralco 4703, 650 K rated) (Fig. 5(c)). The sapphire microsphere was first inserted through *hole-2* on the actuation cantilever and rested on the contact cantilever underneath. It was then fixed to the contact cantilever by applying thermally conductive epoxy around the microsphere-cantilever contact point (Fig. 5(d)). The heat sink was placed on top of the actuation cantilever. The structures were aligned by matching the center hole of the heat sink with the microsphere. The heat sink was then secured by thermally conductive epoxy (Fig. 5(e)). The flatness of the cantilevers was maintained during the assembly process by monitoring the tip height by a high resolution laser displacement sensor (Keyence LK-G32, 50 nm resolution) and adjusting to ensure that the cantilever tip was at the desired height from the ground electrode during epoxy curing. It is envisioned that in the long term, this process can be replaced by a precision pick-and-place process, or eliminated entirely by a lithographic manufacturing method.

A total of nine devices were fabricated and assembled. The distribution is as follows: four devices (two with SS316L contact cantilever and two with Pt–Rh contact cantilever) were used for electrical characterization; two devices (both with Pt–Rh contact cantilevers) were used for thermal characterization; two devices

Please cite this article in press as: F.M. Ozkeskin, Y.B. Gianchandani, Micromachined Pt–Rh and stainless steel relays for high power DC applications, Sens. Actuators A: Phys. (2012), doi:10.1016/j.sna.2011.12.033

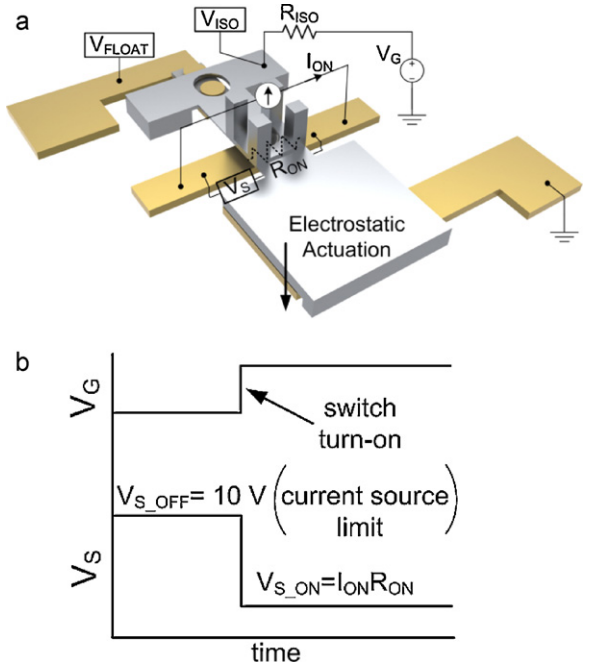


**Fig. 6.** (a) Circuitry for device testing, using actuation voltage ($V_G$) and line current ($I_{ON}$) inputs. (b) Actuation concept showing $V_{S-OFF}$ and $V_{S-ON}$ conditions. $V_{FLOAT}$ is always near 0, whereas $V_{ISO}$ is equal to $V_G$.

(one with SS316L contact cantilever and one with Pt–Rh contact cantilever) were used for energy dispersive X-ray spectroscopy (EDX); and one device (with Pt–Rh contact cantilever) was used for a preliminary measurement of hysteresis and lifetime.

## 4. Experimental evaluation

### 4.1. Electrical testing

The test circuit and the actuation concept for the micro-relay are shown in Fig. 6(a). The inputs include the actuation voltage ($V_G$), the electrical ground, and the line current ($I_{ON}$), which is separately supplied by a current source (limited to 10 V compliance). In figure, framed voltages represent indicators. The isolation of the actuation cantilever is monitored by $V_{ISO}$. Under normal operation there is no current flow across isolation resistor, $R_{ISO}$ (20 kΩ), which is placed between $V_G$, the cantilever actuation voltage supply, and the actuation cantilever. Therefore, in the absence of a short-circuit, $V_G$ and $V_{ISO}$ are normally the same (Fig. 6(b)). If the actuation cantilever is shorted to the contact cantilever or to the ground electrode, a leakage current will generate a voltage drop across $R_{ISO}$, hence result in a $V_{ISO}$ lower than $V_G$. Similarly, $V_{FLOAT}$ is monitored for voltage fluctuations in the floating anchor pad. $V_S$ is used to extract the total series on-state resistance, $R_{ON}$. When the micro-relay is off, $V_S$ is 10 V due to the current source limit (and is denoted by $V_{S-OFF}$). When the device is turned on, $V_S$ is reduced sharply (and is denoted by $V_{S-ON}$). $R_{ON}$ can be extracted from $V_{S-ON}$ by dividing it by $I_{ON}$. $R_{ON}$ is a sum of the contact resistance, cantilever resistance and resistance of the signal lead transfer points at the anchor regions.

The tests were conducted in nitrogen ambient (50.7 kPa vacuum) and repeated for both Pt–Rh and SS316L devices. The electrical tests were intended primarily at determining the maximum power handling allowed by the materials and structure.

Vertical displacement at the tip of the actuation cantilever was recorded using Keyence LK-G32 laser displacement sensor. The voltage was swept from 0 V to 170 V and back to 0 V to observe the hysteresis (Fig. 7). The typical pull-in voltage was around 130 V,

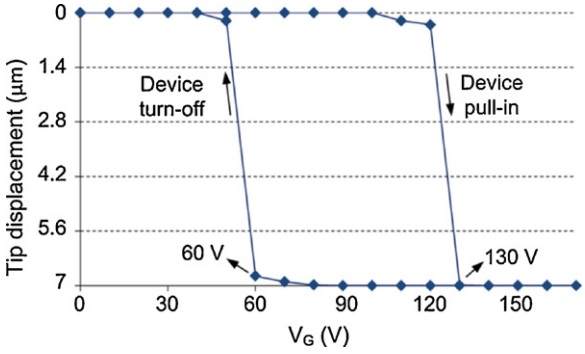


**Fig. 7.** Switching sequence showing the hysteresis. Vertical displacement at the tip of the actuation cantilever was recorded using a laser displacement sensor with 0 V–170 V–0 V actuation voltage sweep. Device pull-in and turn-off voltages were 130 V and 60 V, respectively. The combined stiffness of pair of cantilevers, heat sink and the microsphere, extracted from these measurements, was 70.8 N/m.

slightly larger than the designed value of 120 V. The switching times were approximately 14–15 ms, in good agreement with the pull-in model. The turn-off voltage was typically 60 V; this was used to determine the device spring constant. During the release, electrostatic force and mechanical restoring force are equal in magnitude, assuming van der Waals adhesion forces are neglected and there is no self actuation. The spring constant can then be extracted using following equation [5]:

$$F_{el} = F_k \Rightarrow k = \frac{1}{2}\frac{\varepsilon_0 W w {V_{off}}^2}{g^2 x} \quad (4)$$

where $\varepsilon_0$ is the vacuum permittivity ($8.85 \times 10^{-12}$), $W$ and $w$ are length (1200 μm) and width (1100 μm) of the pull-in electrode, respectively. $V_{off}$ is the turn-off voltage (60 V), $g$ is the electrode gap at pull-in (typically 3–5 μm) and $x$ is the cantilever tip displacement (≈6–8 μm). The resulting spring constant was 70.8 N/m. This value was somewhat larger than the simulated spring constant of 56 N/m.

The change of on-state resistance, $R_{ON}$, with actuation voltage is shown in Fig. 8. Increasing $V_G$ increased the actuation force and reduced on-state resistance, e.g. 1.4 Ω at 140 V, for Pt–Rh contacts, reduced to 1.25 Ω at 160 V. On-state resistance did not decrease significantly past 160 V. Overall, Pt–Rh devices exhibited lower on-state resistances than stainless steel devices, probably due to lower electrical resistivity of the Pt–Rh (≈23 μΩ cm) compared to SS316L (74 μΩ cm). The on-state resistances of devices with the same contact metal exhibited only minimal variations (on the order of 10 mΩ) from device-to-device. On-state resistances were also monitored with changing line current (Fig. 9). For this, $V_G$ was kept constant at 150 V and $I_{ON}$ was increased in 100 mA increments to

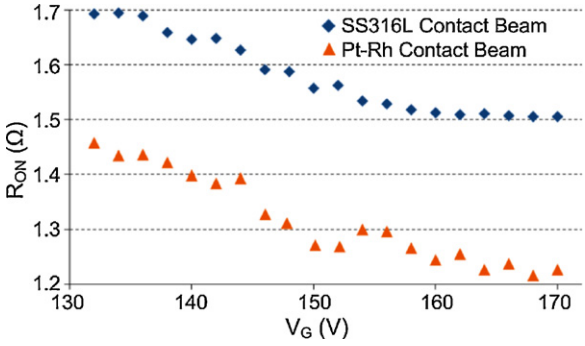


**Fig. 8.** Experimental results showing change of on-state resistance with actuation voltage. Line current $I_{ON}$ was kept constant at 1 A. Increase of $V_G$ yielded higher contact force on signal line hence lower on-state resistance. Pt–Rh devices accommodated lower on-state resistance.

Please cite this article in press as: F.M. Ozkeskin, Y.B. Gianchandani, Micromachined Pt–Rh and stainless steel relays for high power DC applications, Sens. Actuators A: Phys. (2012), doi:10.1016/j.sna.2011.12.033

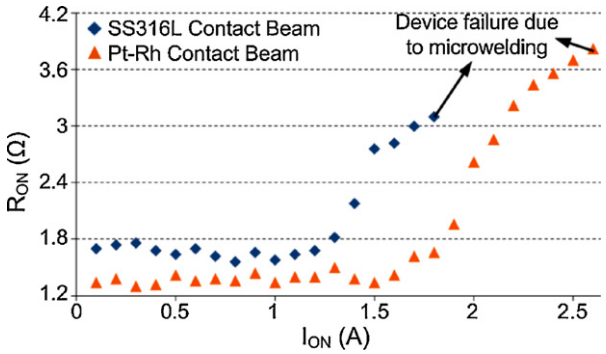


**Fig. 9.** On-state resistance derived from *I–V* curve. $R_{ON}$ is shown for a contact line current up to 2.6 A (in 50.7 kPa nitrogen, unforced cooling). Actuation voltage $V_G$ was maintained constant at 150 V. Resistances augmented sharply past 1.2 A and 1.5 A of $I_{ON}$ for SS316L and Pt–Rh contacts respectively due to softening at contact asperities. Microwelding failures due to localized heating occurred at 1.8 A and 2.6 A for SS316L and Pt–Rh devices, respectively.

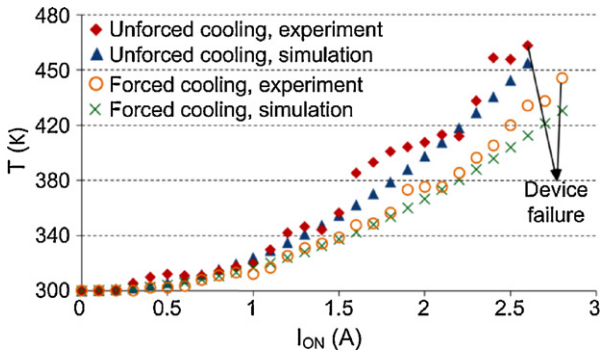


**Fig. 10.** Contact temperature for the Pt–Rh micro-relays subjected to unforced and forced cooling in vacuum nitrogen (50.7 kPa) after 1-s on-state operation at varying current levels. Experimental data was compared with simulations. Device failure due to microwelding occurred at 2.6 A and 2.8 A for unforced and forced cooling, respectively. Heat management with upward forced cooling (compatible with Sunon UF3A3 mini fan, 10 mm × 10 mm × 3 mm size, 0.22 m/s air flow) yielded lowest temperature.

the point of failure. The $R_{ON}$ did not display major change up to 1.2 A line current for SS316L and 1.5 A line current for Pt–Rh devices. Past these points, resistances for both devices sharply increased. Device failures associated with microwelding occurred at 1.8 A and 2.6 A for SS316L and Pt–Rh contacts, respectively.

### 4.2. Thermal testing

Thermal tests included evaluation of Pt–Rh micro-relays under unforced and forced air cooling conditions. A preliminary

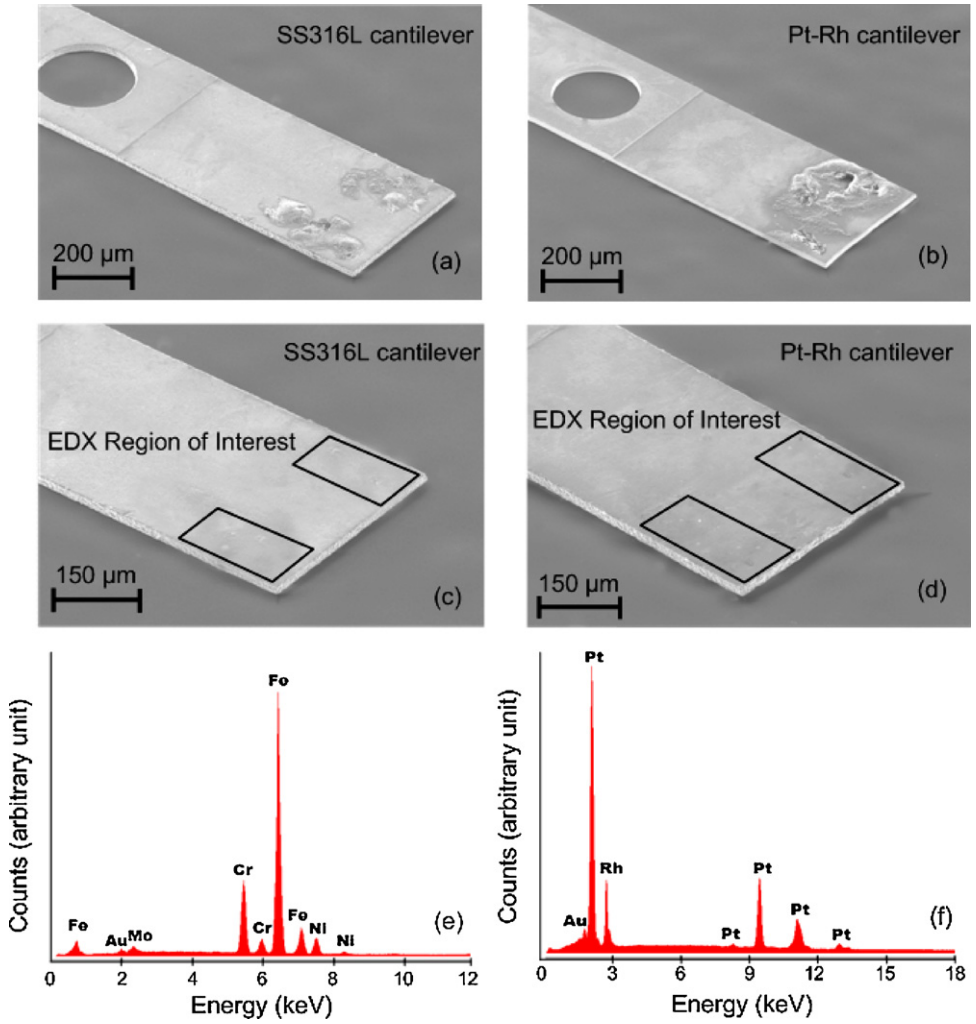


**Fig. 11.** SEM micrographs of failed contact cantilevers after disassembly (view from below). Excessive local heating due to high current yielded metal transfer of PCB material on (a) stainless steel and (b) Pt–Rh contacts at 1.8 A and 2.6 A of line current, respectively, and in 50.7 kPa vacuum nitrogen. Energy dispersive X-ray spectroscopy (EDX) was performed on contact cantilevers after 50 operation cycles at 1 A current. The regions of interest for averaged EDX spectroscopy were 75 μm × 150 μm and enclosed the particles shown on SEM micrographs (c) and (d). EDX spectra for (e) stainless steel and (f) Pt–Rh contacts showed presence of gold.

Please cite this article in press as: F.M. Ozkeskin, Y.B. Gianchandani, Micromachined Pt–Rh and stainless steel relays for high power DC applications, Sens. Actuators A: Phys. (2012), doi:10.1016/j.sna.2011.12.033

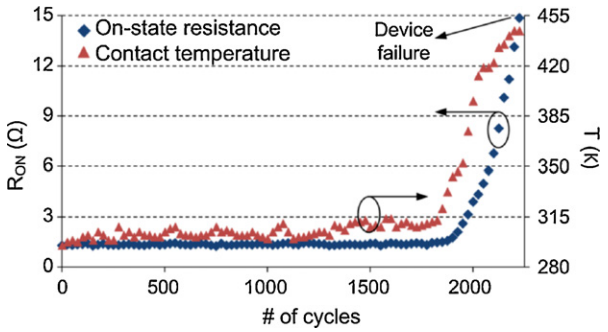


**Fig. 12.** Lifetime characterization of the micro-relay. The test was run under hot switching conditions in nitrogen (50.7 kPa) with 1 A line current and 160 V actuation voltage. The frequency was 0.5 Hz and duty cycle was 50%. A drastic change in on-state resistance was observed past 1900 cycles leading to failure in the 2226th cycle. The corresponding contact temperatures are also shown. At device failure the contact temperature recorded was 443 K.

assessment of the thermal conditions for the Pt–Rh micro-relay was performed by measuring the contact temperature at the end of each 1-s actuation time period during which varying levels of current were maintained. Tests were performed in 50.7 kPa nitrogen for both unforced and forced cooling cases. A constant actuation voltage, $V_G$, of 150 V was applied during the tests.

The measurements were performed with the T type Perfluoroalkoxy (PFA) insulated thermocouple (OMEGA Inc., 15 cm length, 70 μm exposed tip diameter); the manufacturer-specified thermocouple tolerance was ±0.5 K. For measurements, the tip of the thermocouple wire was brought in close proximity to the contact area and pressed against the signal line. The room temperature was 300 K during these tests. For forced cooling experiments the mini-fan was located approximately 1 mm above the device. The flow was forced upward from the device. (The flow rate was not experimentally verified at the operating pressure of 50.7 kPa. As noted previously, the flow velocity at atmospheric pressure was 0.22 m/s.)

Typical measurements for contact area temperatures (following 1-s into the on-state) of the Pt–Rh micro-relay are shown in Fig. 10. The impact of forced cooling is evident, e.g. for 2 A line current, unforced cooling on the micro-relay resulted in 408 K contact temperature, whereas forced cooling suppressed contact temperature rise by at least 20 K. Devices with forced cooling exhibited higher current handling (2.8 A).

Micro-relays were disassembled after failure and contact cantilevers surfaces were observed (Fig. 11(a) and (b)). Pt–Rh and SS316L cantilevers were microwelded on Au–Ni–Cu layers of PCB due to excessive heating at the contact asperities. Surface material conditions for another pair of contact cantilevers were observed using EDX after only 50 operation cycles at 1 A electrical current, well before failure (Fig. 11(c) and (d)). For averaged EDX spectroscopy, regions of interests were chosen as boxes (75 μm × 150 μm) over contact areas. Both SS316L and Pt–Rh contact cantilevers displayed small traces of gold, indicating material transfer in the initial cycles, even at lower powers (Fig. 11(e) and (f)).

### 4.3. Lifetime testing

A preliminary evaluation of lifetime of the Pt–Rh micro-relays was performed under hot switching conditions. An electrical line current of 1 A was used and an actuation voltage of 160 V was maintained for the test. The micro-relay was operated at 0.5 Hz frequency with 50% duty cycle. The test was done in nitrogen (50.7 kPa) with the mini-fan kept on all the time. The on state resistance, $R_{ON}$, was recorded until the device failure occurred. Contact temperatures were also recorded as described in the previous section.

Lifetime test results are shown in Fig. 12. The micro-relay operated 2226 cycles before failure. Since the devices were actuated a few tens of times for assembly check purpose before the actual lifetime test, $R_{ON}$ did not exhibit a change for the initial cycles and was constant at 1.2–1.4 Ω for approximately 1900 cycles. A drastic increase in the on-state resistance was observed past 1900 cycles and $R_{ON}$ was approximately 15 Ω at failure. The figure also shows the contact temperature, which remained stable below 2000 cycles, but sharply increased past 440 K near the point of failure.

## 5. Discussion and conclusions

Electrostatically actuated micro-relay test structures for high power DC applications were evaluated in this paper. Pt–Rh alloy bulk foil was evaluated as the structural contact material for its inert nature and its resistance to softening and wear. The contact metal to mate with Pt–Rh was Au because of its widespread use in PCB manufacturing. A contact pair solely based on Pt-group metals is expected to be susceptible to frictional polymerization, i.e. the formation of a contaminant film due to absorption of organic vapor from the air under fretting conditions with shear or normal force [26,28]. The use of Au with Pt-group metals is known to alleviate the effects of this phenomenon significantly [29]. EDX spectroscopy suggests that some portion of Au top layer is transferred onto contact cantilevers after 50 operation cycles with 1 A electrical current. This phenomenon indicates that contacting SS316L/Pt–Rh and Au pairs potentially contributes to the net reduction of contact resistance.

As noted in Section 4, during normal operation, the on-state resistance, $R_{ON}$, was a sum of the contact resistance, cantilever resistance and resistance of the signal lead transfer points at the anchor regions. At high currents (>1 A), the measured on-state resistances were approximately 1.5 Ω and 1.25 Ω for SS316L and Pt–Rh micro-relays, respectively. Measured on-state resistances were higher than both $R_{C\_theory}$ and $R_{C\_emp}$. This is likely due to the parasitic resistances contributed by the cantilever and transfer points, as noted above. Overall, the on-state resistance of the micro-relays was higher when compared to DC relays intended for low power handling. In one case, a 1 Ω contact resistance was reported for an 80 mA current [1]; in another case a 35 mΩ contact resistance was reported for 20 mA [12].

Failures due to localized heating occurred at 1.8 A and 2.6 A for SS316L and Pt–Rh devices, respectively. The early failure of SS316L micro-relays compared to Pt–Rh micro-relays has two likely reasons. First, the larger electrical resistivity of SS316L leads to greater joule heating, which, in turn, increases the temperature that contributes to failure. Second, the thermal conductivity of SS316L is about 16 W/m K whereas that of Pt–Rh is approximately 35 W/m K [30]. Therefore, the contact temperature for SS316L micro-relays is higher than for Pt–Rh micro-relays, which, in turn, increases the on-state resistance and contributes to an earlier failure. Pt–Rh devices with forced cooling exhibited a current rating of 2.8 A in 50.7 kPa nitrogen. The use of forced cooling suppressed contact temperature rise by approximately 20 K. The relatively modest nature of this improvement suggests that the added complexity of the heat sink is not justified for the conditions evaluated in this paper.

An unpackaged Pt–Rh micro-relay operated for 2226 cycles under hot switching conditions of 1 A line current. This is approximately 10× greater than other high current DC micro-relays tested at about 100 mA [31]. It is expected that device packaging can further extend the device lifetime.

The test structures evaluated in this study were relatively compact compared to the packaged solid state relays. The current

Please cite this article in press as: F.M. Ozkeskin, Y.B. Gianchandani, Micromachined Pt–Rh and stainless steel relays for high power DC applications, Sens. Actuators A: Phys. (2012), doi:10.1016/j.sna.2011.12.033

**Table 1**
Device performance summary. Fabricated devices provide small footprint and high current handling.

| Property | Contact metal | |
|---|---|---|
| | SS316L | Pt–Rh |
| Footprint ($mm^2$) | 6.5 (2.6 × 2.5) | |
| Actuation area ($mm^2$) | 1.32 (1.2 × 1.1) | |
| Maximum current (A) | 1.8 | 2.8 |
| On resistance (Ω) | 1.5 | 1.2 |
| Actuation time (ms) | 10–15 | |

handling was 2–3 times higher than that reported for other DC micro-relays of similar size [10,12]. However, on-state resistances were high and actuation times were slow (Table 1).

This work has demonstrated the possible utility of bulk metal foils as candidates for high power contact relays. The main goal of this effort has been to evaluate the power limits of such relays. Future efforts may be directed at adapting the structure for automated pick-and-place assembly or other format of batch-mode mass production; extending the functionality to high power RF switching; and device packaging.

## Acknowledgement

This study is supported in part by Defense Advanced Research Projects Agency, Microsystems Technology Office (DARPA MTO) contract # W31P4Q-09-1-0009.

## References

[1] Z.H. Li, D.C. Zhang, T. Li, W. Wang, G. Wu, Bulk micromachined relay with lateral contact, Journal of Micromechanics and Microengineering 10 (September) (2000) 329–333.
[2] Y. Liu, Y. Li, T. Abe, Y. Haga, M. Esashi, A thermomechanical relay with microspring contact array, in: Proc. 14th IEEE International Conference on Micro Electro Mechanical Systems (MEMS'01), Interlaken, Switzerland, 2001, pp. 220–223.
[3] L. Almeida, R. Ramadoss, R. Jackson, K. Ishikawa, Q. Yu, Laterally actuated multicontact MEMS relay fabricated using MetalMUMPS process: experimental characterization and multiscale contact modeling, Journal of Micro/Nanolithography, MEMS, and MOEMS 6 (June) (2007), 023009-1-10.
[4] S. Lucyszyn, Review of radio frequency microelectromechanical systems technology, IEEE Science, Measurement & Technology 151 (2004) 93–103.
[5] G.M. Rebeiz, RF MEMS: Theory, Design and Technology, John Wiley and Sons, Hoboken, NJ, 2003.
[6] C.B. Jacobina, I.S.D. Freitas, E.R.C.D. Silva, A.M.N. Lima, R.L.D.A. Ribeiro, Reduced switch count DC-link AC–AC five-leg converter, IEEE Transactions On Power Electronics 21 (September) (2006) 1301–1310.
[7] B. Norvell, R. Hancock, J. Smith, M. Pugh, S. Theis, J. Kviatkofsky, Micro electro mechanical switch (MEMS) technology applied to electronically scanned arrays for space based radar, in: Proc. IEEE Aerospace Conference, Aspen, CO, 1999, pp. 239–247.
[8] B.D. Jensen, L.L.W. Chow, K. Huang, K. Saitou, J.L. Volakis, K. Kurabayashi, Effect of nanoscale heating on electrical transport in RF MEMS switch contacts, Journal of Microelectromechanical Systems 14 (October) (2005) 935–946.
[9] H. Kwon, D.-J. Choi, J.-H. Park, H.-C. Lee, Y.-H. Park, Y.-D. Kim, H.-J. Nam, Y.-C. Joo, J.-U. Bu, Contact materials and reliability for high power RF-MEMS switches, in: Proc. 20th IEEE International Conference on Micro Electro Mechanical Systems (MEMS'07), Hyogo, Japan, 2007, pp. 231–234.
[10] W.P. Taylor, O. Brand, M.G. Allen, Fully integrated magnetically actuated micromachined relays, Journal of Microelectromechanical Systems 7 (December) (1998) 181–191.
[11] H.S. Lee, C.H. Leung, J. Shi, S.C. Chang, Electrostatically actuated copper-blade microrelays, Sensors and Actuators A 100 (August) (2002) 105–113.
[12] J.-E. Wong, J.H. Lang, M.A. Schmidt, An electrostatically actuated MEMS switch for power applications, in: Proc. 13th IEEE International Conference on Micro Electro Mechanical Systems (MEMS'00), Miyazaki, Japan, 2000, pp. 633–638.
[13] R.A. Coutu, P.E. Kladitis, K.D. Leedy, R.L. Crane, Selecting metal alloy electric contact materials for MEMS switches, Journal of Micromechanics and Microengineering 14 (August) (2004) 1157–1164.
[14] N.E. Mcgruer, G.G. Adams, L. Chen, Z.J. Guo, Y. Du, Mechanical, thermal, and material influences on ohmic-contact-type MEMS switch operation, in: Proc. 19th IEEE International Conference on Micro Electro Mechanical Systems (MEMS'06), Istanbul, Turkey, 2006, pp. 230–233.
[15] H.R. Lee, A. Coutu, S. Mall, K.D. Leedy, Characterization of metal and metal alloy films as contact materials in MEMS switches, Journal of Micromechanics and Microengineering 16 (March) (2006) 557–563.
[16] L. Chen, H. Lee, Z.J. Guo, N.E. McGruer, K.W. Gilbert, S. Mall, K.D. Leedy, G.G. Adams, Contact resistance study of noble metals and alloy films using a scanning probe microscope test station, Journal of Applied Physics 102 (October) (2007), 074910:1-7.
[17] S. Majumder, J. Lampen, R. Morrison, J. Maciel, A. Packaged, High-lifetime ohmic MEMS RF switch, in: IEEE MTT-S Microwave Symposium Dig., Philadelphia, PA, 2003, pp. 1935–1938.
[18] S. Duffy, C. Bozler, S. Rabe, J. Knecht, L. Travis, P. Wyatt, C. Keast, M. Couker, MEMS microswitches for reconfigurable microwaves circuitry, IEEE Microwave and Wireless Components Letters 11 (March) (2001) 106–108.
[19] G. Dereli, T. Cagin, M. Uludogan, M. Tomak, Thermal and Mechanical Properties of Pt–Rh Alloys, Philosophical Magazine Letters 75 (November) (1997) 209–217.
[20] B. Fischer, A. Behrends, D. Freund, D.F. Lupton, J. Merker, High temperature mechanical properties of the platinum group metals, Platinum Metals Review 43 (January) (1999) 18–28.
[21] F.M. Ozkeskin, Y.B. Gianchandani, Double-cantilever micro-relay with integrated heat sink for high power applications, in: PowerMEMS2010 Conference, Leuven, Belgium, 2010, pp. 159–162.
[22] F.M. Ozkeskin, Bulk Foil Pt-Rh Micro-relays for High Power RF and Other Applications. Ph.D. Thesis. University of Michigan, 2011.
[23] R. Holm, Electric Contacts, Springer-Verlag, Berlin, Germany, 1968.
[24] P.G. Slade (Ed.), Electrical Contacts: Principles and Applications, Marcel Dekker, New York, 1999.
[25] F.P. Bowden, D. Tabor, Friction and Lubrication of Solids, vol. 2, Oxford University Press, Oxford, UK, 1964.
[26] M.B. Read, J.H. Lang, A.H. Slocum, Contact resistance in flat thin films, in: Proc. 55th IEEE Holm Conference on Electrical Contacts, 2009, pp. 303–309.
[27] K. Takahata, Y.B. Gianchandani, Batch mode micro-electro-discharge machining, Journal of Microelectromechanical Systems 11 (April) (2002) 102–110.
[28] W.H. Abbott, W.K. Campbell, Frictional polymer formation on precious metals. Experimental observation, in: Proc. 9th International Conference on Electrical Contact Phenomena, Chicago, IL, 1978, pp. 359–363.
[29] M. Antler, The application of palladium in electronic connectors, Platinum Metals Review 26 (July) (1982) 106–117.
[30] E. Preston, Platinum in the glass industry, Platinum Metals Review 4 (January) (1960) 2–9.
[31] J.-M. Kim, S. Lee, C.-W. Baek, Y. Kwon, Y.-K. Kim, Cold- and hot switching lifetime characterizations of ohmic-contact RF MEMS switches, IEICE Electronics Express 5 (June) (2008) 418–423.

## Biography

**Fatih M. Ozkeskin** received his B.S. degree in mechatronics engineering from Sabanci University, Turkey in 2006 and his M.S. degree in mechanical engineering from Texas A&M University in 2008. He received both his M.S. degree in electrical engineering and his Ph.D. degree in mechanical engineering from University of Michigan, Ann Arbor in 2011. He is currently a process engineer at Applied Materials, Santa Clara, CA. His research interests include MEMS switches and micro/nano manufacturing.

Please cite this article in press as: F.M. Ozkeskin, Y.B. Gianchandani, Micromachined Pt–Rh and stainless steel relays for high power DC applications, Sens. Actuators A: Phys. (2012), doi:10.1016/j.sna.2011.12.033